View Online

Mesoporous metallo-silicates as a support of cobalt catalysts for slurry phase Fischer–Tropsch synthesis

Mingdeng Wei,*[a] Kiyomi Okabe,[a] Hironori Arakawa[a] and Yasutake Teraoka[b]

[a] *National Institute of Advanced Industrial Science and Technology, Tsukuba Central #5, Ibaraki 305-8565, Japan. E-mail: wei-mingdeng@aist.go.jp; Fax: + 81 29 861 4487*
[b] *Department of Molecular and Material Science, Graduate of School of Engineering Sciences, Kyushu University, Fukuoka 816-8580, Japan*

Received (in New Haven, CT, USA) 7th January 2003, Accepted 26th January 2003
First published as an Advance Article on the web 8th May 2003

Published on 08 May 2003 on http://pubs.rsc.org | doi:10.1039/B300723P
Downloaded on 26 October 2010

A series of mesoporous metallo-silicates (M-MPS, M = Al, Mn, V, Zr, and Mo) was synthesized at ambient temperature by utilizing hexadecylpyridinium chloride as a surfactant and was used as the support of cobalt catalysts for Fischer–Tropsch synthesis in a slurry phase. The catalysts supported on M-MPS showed a higher selectivity for C_{5+} hydrocarbons and had a higher chain growth probability α, as well as a lower selectivity for CH_4. A good correlation between the selectivity for CH_4 and the standard enthalpy of formation of metal oxides incorporated into the silica framework, $-\Delta H_f^0$, was obtained and the role of metals incorporated into the silica framework in Fischer–Tropsch synthesis is discussed.

Introduction

Since the important breakthrough of the discovery of M41S materials,[1] most of the further studies have been focused on the hexagonal MCM-41 materials. However, the purely siliceous MCM-41 showed limited catalytic applications. Therefore, incorporation of metal centers in the silica framework is necessary for their use in catalysis. Several elements, including Al,[2] Ti,[3] V,[4] Mo,[5] Zr,[6] Mn,[7] Fe,[8] Co,[8] Cr,[9] La,[10] Ce,[11] B[12] and Ga[12] have been reported to be incorporated into the framework in order to generate catalytic activity. Up to now, use of the purely siliceous MCM-41 as a support of Co catalysts for Fischer–Tropsch (F–T) synthesis has been reported.[13–16] However, the reports on F–T synthesis over Co catalysts supported on mesoporous metallo-silicates are limited.[17]

In this study, a series of mesoporous metallo-silicate materials (M-MPS; M = Al, Mn, V, Zr and Mo) was synthesized and their crystal structure and physical properties were determined by powder X-ray diffraction (XRD), N_2 adsorption-desorption and FT-IR. These materials were used as a support of Co catalysts for F–T synthesis in a slurry phase and the effects of the metals incorporated into the silica framework on the catalytic activity and the selectivity were investigated. Furthermore, the role of metals incorporated into the silica framework in F–T synthesis is discussed.

Experimental

Chemicals

Hexadecylpyridinium chloride (C_{16}PyCl, Kanto Chemical Co., Inc.) was selected as the surfactant and sodium silicate ($Na_2{\cdot}2SiO_2{\cdot}nH_2O$, Kishida) was used as the Si source. The inorganic precursors, $Al(NO_3)_3{\cdot}9H_2O$, $Mn(NO_3)_2{\cdot}6H_2O$, $ZrO(NO_3)_2{\cdot}2H_2O$, NH_4VO_3, $(NH_4)_6Mo_7O_{24}{\cdot}2H_2O$, $Co(NO_3)_2{\cdot}6H_2O$ and $IrCl_4{\cdot}H_2O$, were obtained from Wako Co., Ltd.

Synthesis of mesoporous metallo-silicates

Hexadecylpyridinium chloride (C_{16}PyCl) was used as the cationic surfactant in the synthesis of metal-containing mesoporous silicate materials.[17, 18] The typical procedure is as follows: C_{16}PyCl (3.0 mmol) was dissolved in 52 ml of water. With vigorous stirring and optional heating, appropriate amounts of HCl and NaOH, in a molar ratio of (Si + M): Surf.:NaOH:HCl:H_2O = 1:0.12:1.06–1.27:0.61:141, were added in order to adjust the pH value of the surfactant solution below or above 11, respectively. Clear solutions of the required amount of sodium silicate and metal salts were added dropwise into the surfactant solution at room temperature with vigorous stirring. After further stirring for 3 h at room temperature, the precipitate was filtered, washed thoroughly with water, dried in an oven at 110 °C for 6 h, and finally calcined in air at the appropriate temperature for 6 h in order to remove the template.

Preparation of Co catalysts supported on mesoporous materials

The required amounts of $Co(NO_3)_2{\cdot}6H_2O$ and $IrCl_4{\cdot}H_2O$ were dissolved in de-ionized water, and then dispersed completely onto the mesoporous materials using the impregnation method. The obtained solid mixture was calcined at 350 °C for 1 h in order to decompose any remaining nitrate.

Characterization of mesoporous materials and catalysts

X-Ray powder diffraction (XRD) patterns were recorded using a Mac Science MPX-18 diffractometer. Multi-point BET surface area, pore volume and BJH pore size distribution of materials were calculated from the adsorption-desorption isotherm of N_2 at 77 K (Micromeritics, ASAP 2000). FT-IR spectra were measured using a Digilab FTS-60 instrument.

Fischer–Tropsch reaction

After reduction at 400 °C for 15 h in H_2 flow, the catalyst (2 g) was suspended in 50 ml of *n*-hexadecane. The F–T reaction was carried out with the catalyst slurry in an autoclave-type semi-batch reactor (flow type for gas phase), whose volume was approximately 100 ml. The feed gas (H_2:CO:Ar = 60:30:10) was bubbled into the slurry and the dissolution of

 DOI: 10.1039/b300723p

This journal is © The Royal Society of Chemistry and the Centre National de la Recherche Scientifique 2003

View Online

Published on 08 May 2003 on http://pubs.rsc.org | doi:10.1039/B300723P
Downloaded on 26 October 2010

the gas into the slurry was promoted by a specially designed stirring rod.[19] The reaction conditions were as follows: $T = 230\,^{\circ}C$, $P = 1$ MPa and W/F = 10 g catal·h·mol^{-1}. The effluent gas was periodically analyzed by using Shimadzu on-line gas chromatographs (models 14B and 17A) with TCD and FID detectors, while the amounts of inorganic gases and C_{1-14} hydrocarbons were quantified using the Ar in the sample gas as an internal standard. The C_{10+} hydrocarbons in the slurry were determined separately by gas chromatography after the reaction.

Results and discussion

Synthesis and characterization of mesoporous metallo-silicates

The XRD patterns of metal-containing mesoporous silicates (M-MPS; M = Al, Mn, V, Zr, and Mo) with a Si:M ratio of 29 as well as mesoporous silica (MPS) synthesized by the same method[18] are depicted in Fig. 1. All three XRD reflections, (100), (110) and (200), are resolved and can be indexed to a hexagonal lattice, indicating that these materials are structurally analogous to MCM-41.[1] The peak distortion varies when different metals are incorporated into silica framework. The peak intensities of M-MPS samples become broader and less intense, as shown in Fig. 1. Therefore, the maximum content of metals incorporated into the silica framework with a mesoporous structure is limited. For example, when the Si:Al ratio of the starting mixture is below 19, the distortion is very significant. So we suggest that the highest content of Al incorporated into the silica framework is *ca.* 5 mol %. When metals are incorporated into the silica framework, the spacing of the (100) diffraction shifts from the 3.2 nm found in purely siliceous MPS to a range of 3.3–3.6 nm for M-MPS materials. It was reported that the d_{100} spacing decreased when Mo is incorporated into silica framework .[5] However, we observed the opposite behavior.

The effect of the incorporation of metals into the silica framework is clearly indicated by the changes in the thickness of the pore walls (calculated by subtracting the pore diameter from the unit cell parameter). The thickness of the pore wall increases from the 1.2 nm found in the purely siliceous MPS to 1.4–1.9 nm in M-MPS materials. The purely siliceous MPS exhibits the highest surface area at 1217 m^2 g^{-1}, which decreases to some extent upon incorporation of metals into the framework to form M-MPS materials (see Table 1).

Table 1 The physical properties of metal-containing mesoporous materials (Si:M = 29)

Sample	d_{100} spacing/ nm	S_{BET}/ m^2 g^{-1}	Pore volume/ cm^3 g^{-1}	Unit cell parameter[a]/ nm	Wall thickness/ nm
MPS	3.2	1217	0.82	3.7	1.2
Al-MPS	3.5	957	0.78	4.0	1.5
Mn-MPS	3.3	830	0.67	3.8	1.4
V-MPS	3.4	956	0.84	3.9	1.6
Zr-MPS	3.5	1082	0.83	4.0	1.9
Mo-MPS	3.6	949	0.76	4.2	1.7

[a] Unit cell parameter = $(2/\sqrt{3})\cdot d_{100}$ = pore diameter + wall thickness

The N_2 adsorption-desorption isotherms of MPS and M-MPS exhibit an isotherm of type IV with three stages of adsorption (Fig. 2). The $P/P_0 < 0.2$ stage is attributed to monolayer adsorption of nitrogen on the walls of mesopores. The $0.2 < P/P_0 < 0.35$ stage with a sharp step is due to capillary condensation inside the mesopores, corresponding to a characteristic of MCM-41 type ordered mesoporous materials.[20] Except for MPS, the other materials show well-expressed hysterisis loops in the $P/P_0 > 0.9$ stage, corresponding to capillary condensation in a textural or interparticle mesoporosity.[21] The position of the inflection in the $0.2 < P/P_0 < 0.35$ stage depends on the diameter of the mesopores and its sharp step indicates the uniformity of the narrow pore size distribution. The inflection position varies with different types and content of metal incorporated into the framework.

The FT-IR spectra of MPS and M-MPS are given in Fig. 3. In all cases, an IR band at *ca.* 970 cm^{-1} is observed. Such a

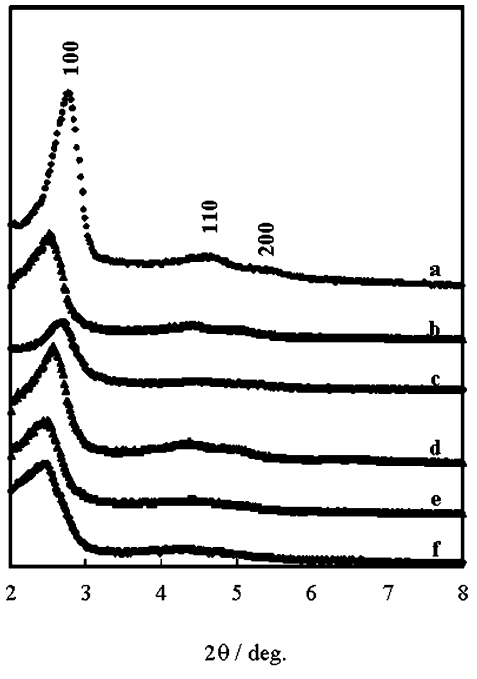

Fig. 1 Powder XRD patterns of (a) MPS, (b) Al-MPS, (c) Mn-MPS, (d) V-MPS, (e) Zr-MPS and (f) Mo-MPS. Si:M = 29.

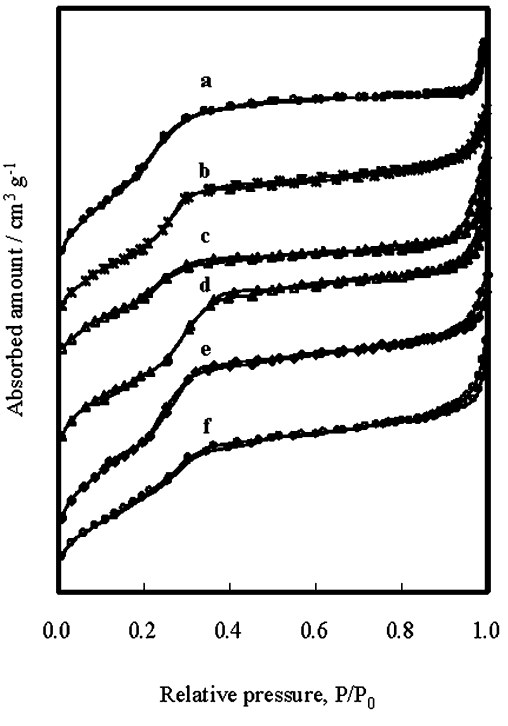

Fig. 2 N_2 adsorption-desorption isotherms at 77 K of (a) MPS, (b) Al-MPS, (c) Mn-MPS, (d) V-MPS, (e) Zr-MPS and (f) Mo-MPS. Si:M = 29.

View Online

Published on 08 May 2003 on http://pubs.rsc.org | doi:10.1039/B300723P
Downloaded on 26 October 2010

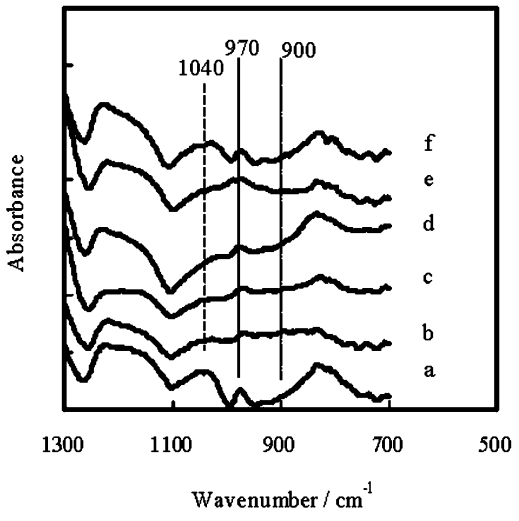

Fig. 3 FT-IR spectra of (a) MPS, (b) Al-MPS, (c) Mn-MPS, (d) V-MPS, (e) Zr-MPS and (f) Mo-MPS. Si:M = 29.

band was usually assigned to the M–O–Si stretching vibration in Ti-,[22] V-,[22] Mo-,[23] Zr-[24] and Mn-containing[7] mesoporous materials. However, the interpretation of this band has been a matter of debate, because a similar band is observed in MCM-41.[25] On the other hand, the asymmetric stretching band at ~1040 cm^{-1} becomes less structured when metals are incorporated. This is taken as an indication of a loss in structural regularity[9] and also agrees with the observed XRD patterns. According to a report by Rana *et al.*,[23] a band at 900 cm^{-1} was assigned to Mo=O vibrations in complexes of the type $(Mo{=}O)^{4+}$, $(Mo{-}OH)^{5+}$ or MoO_4^{2-} bonded to the lattice. However, this band was not observed for our Mo-MPS sample.

Preparation and characterization of Co catalysts supported on mesoporous metallo-silicates

A series of Co catalysts supported on mesoporous metallo-silicates was prepared and characterized by XRD and N_2 adsorption-desorption. For typical samples, V-MPS and a 0.5 wt% Ir–20 wt% Co–V-MPS catalyst showed a narrow pore size distribution (Fig. 4), but the intensity of the latter obviously decreased, indicating a considerable lowering in structural regularity. The surface area decreased from 956 to 704 $m^2\ g^{-1}$ after Co–Ir loading and the pore volume also decreased from 0.84 to 0.61 $cm^3\ g^{-1}$. From these results, we suggest that the metal ions Co^{2+} and Ir^{4+} are effectively deposited onto the inner walls of the mesoporous materials. Similar results were also reported previously.[17]

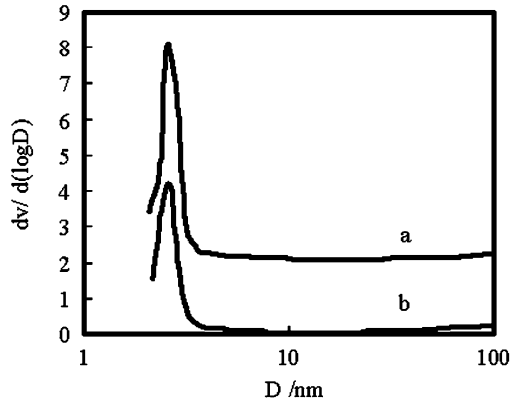

Fig. 4 Pore size distribution of (a) V-MPS and (b) 0.5% Ir–20% Co catalyst supported on V-MPS. Si:V = 29.

F–T synthesis

The F–T synthesis was carried out in a slurry phase over Co–Ir catalysts supported on M-MPS materials (M = Al, V, Mn, Zr, and Mo); the reaction results at the steady state are listed in Table 2. The selectivity for C_{5+} hydrocarbons increased when metals were incorporated. The effects of metals incorporated into the framework on the CO conversion and the selectivity were significantly different, but the catalysts supported on M-MPS tend to increase the fraction of heavy hydrocarbons (C_{5+}) and the chain growth probability α, while the selectivity for CH_4 is effectively restrained.

A series of Co catalysts supported on Al-MPS materials with different ratios of Si:Al was investigated in our previous report[17] and the effect of Al in the silica framework on the catalytic properties was described. Compared with the catalyst supported on mesoporous silica (MPS), the catalyst supported on Al-MPS showed higher selectivity for C_{5+} hydrocarbons and a higher chain growth probability α, while the selectivity for CH_4 decreased slightly. This might be attributed to Al incorporated into the silica framework. The catalysts supported on Mn-, V-, Zr- and Mo-MPS also increase the selectivity for C_{5+} hydrocarbons and the chain growth probability α. However, except for CH_4 selectivity, the distribution of the products and the α value are not significantly different. The addition of light transition metal oxides (LTMO, such as Mn,[26,27] V,[28] Mo[29]) has been explored by several workers and was also reviewed.[30] It was considered that these compounds facilitate CO dissociation at the sites of the metal and promoter interface and lower the surface H:C ratio due to electronic interaction with the metal surface.

Plots of CO conversion as a function of time on stream are shown in Fig. 5. All catalysts showed deactivation at different levels, except for the catalysts supported on Al- and V-MPS. This can be explained by the results of powder XRD of used catalysts, as shown in Fig. 6. Inactive Co_3O_4 was found in the Co catalysts supported on MPS. This might be the reason that the catalyst showed deactivation. No peak was observed in the Co catalyst supported on Al-MPS, indicating that the reduced Co^0 particles were highly dispersed on the support and could not be detected by the XRD measurements (Co particle size < 3 nm). This might be the reason that deactivation was not observed even after a reaction time of more than 55 h. In view of these results, we suggest that the role of Al_2O_3 is to divide the partially active Co sites and to prevent the growth of the Co^0 particle size, resulting in enhancement of the thermal stability of Co catalyst. Co_3O_4, CoO and MnO were detected in the used catalyst supported on Mn-MPS. This might be the reason that this catalyst showed deactivation. In contrast, two kinds of Co metal crystallites, cubic (fcc) and hexagonal (hcp), were found in the used Co catalysts supported on V-, Zr-, and Mo-MPS materials with the cubic phase being predominant. The fcc phase is reported to be an active Co phase in F–T

Table 2 The catalytic activity and the selectivity of F–T synthesis over 0.5 wt % Ir–20 wt % Co catalysts supported on mesoporous metallo-silicates (Si:M = 29, average C%)

Support	$S_{BET}/m^2\ g^{-1}$ (catalyst)	CO conv. (%)	Selectivity (%)				
			CH_4	CO_2	C_{2-4}	C_{5+}	α^a
MPS	663	50.8	14.2	1.1	25.2	59.2	0.76
Al-MPS[b]	481	44.7	11.2	0.5	10.4	73.6	0.88
Mn-MPS	458	46.8	4.5	2.5	15.9	85.1	0.85
V-MPS	704	42.4	9.4	1.2	14.5	80.8	0.85
Zr-MPS	628	44.2	7.1	1.6	13.8	83.7	0.85
Mo-MPS	626	47.3	6.6	2.1	16.3	84.8	0.84

[a] The chain growth probability α was calculated from a Schultz–Flory distribution. [b] Ir content is 1.0 wt %.

View Online

Published on 08 May 2003 on http://pubs.rsc.org | doi:10.1039/B300723P
Downloaded on 26 October 2010

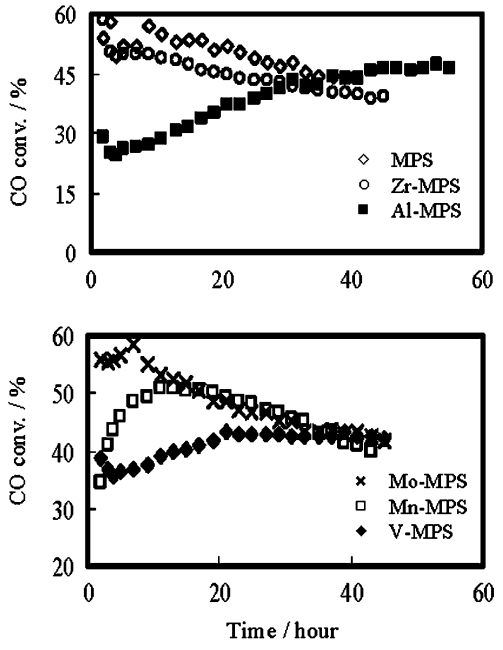

Fig. 5 Time course of the Fischer–Tropsch synthesis in slurry phase over 0.5 wt% Ir–20 wt% Co catalysts supported on MPS and M-MPS with a Si:M ratio of 29 (M = Al, Mn, V, Zr, and Mo)

synthesis.[16] This might explain the fact that these catalysts show a higher selectivity for C_{5+} hydrocarbons and a higher α value with restrained CH_4 selectivity.

In order to elucidate the effect of the metal state in the catalysts on F–T synthesis, three typical metal-promoted catalysts consisting of 0.5 wt % Ir–20 wt % Co–x wt % M (M = Al, Mn and Zr) supported on MPS were used, in which the ratio of Si:M is 29. The results of F–T synthesis are summarized in Table 3. Compared with the results in Table 2, the metal-promoted Co catalysts supported on MPS showed lower selectivity for C_{5+} hydrocarbons and a smaller α value than the corresponding catalysts supported on mesoporous metallosilicates (M-MPS). The difference between the catalysts supported on M-MPS and metal-promoted catalysts supported on MPS is that M in the former is incorporated into the silica framework, forming a tetrahedral coordination with oxygen, while in the latter it is in the form of metal oxides. From these results, we suggest that the metal promoter, highly dispersed in the catalyst (incorporated into the silica framework), contributes to increase the selectivity for heavy hydrocarbons in F–T synthesis.

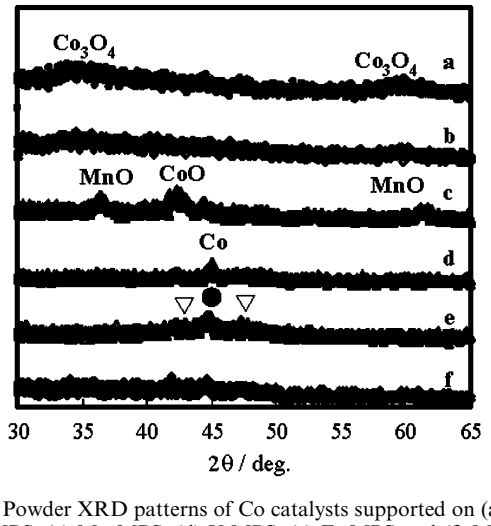

Fig. 6 Powder XRD patterns of Co catalysts supported on (a) MPS, (b) Al-MPS, (c) Mn-MPS, (d) V-MPS, (e) Zr-MPS and (f) Mo-MPS. Si:M = 29. (●) Co(fcc) and (▽) Co(hcp).

Table 3 The catalytic activity and the selectivity of F–T synthesis over 0.5 wt % Ir–20 wt % Co–x wt % M catalysts supported on mesoporous silicate (average C%)

Catalyst[a]	CO conv. (%)	Selectivity (%)				
		CH_4	CO_2	C_{2-4}	C_{5+}	α^b
0.5 wt % Ir–20 wt % Co–1.2 wt % Al/MPS	46.0	11.8	0.7	26.0	72.0	0.78
0.5 wt % Ir–20 wt % Co–2.4 wt % Mn/MPS	50.7	6.7	0.8	19.8	81.3	0.81
0.5 wt % Ir–20 wt % Co–4.2 wt % Zr/MPS	55.1	9.5	1.2	26.1	66.5	0.78

[a] Si/M = 29, M = Al, Mn and Zr. [b] The chain growth probability α was calculated from a Schultz–Flory distribution.

In F–T synthesis, one of the problems is high CH_4 selectivity in the product distribution. Fig. 7 shows the relationship between CH_4 selectivity and the standard enthalpy of formation of metal oxides incorporated into the silica framework, $-\Delta H_f^0$.[31] A good correlation was obtained and the selectivity for CH_4 increases with $-\Delta H_f^0$. The standard enthalpy of formation of metal oxide per oxygen atom, $-\Delta H_f^0$/O atom, is often used as a parameter of metal–oxygen bond strength, the ability to activate oxygen, or the redox properties of metal cations (oxides). Among all the catalysts, the catalyst supported on Mn-MPS shows the lowest selectivity for CH_4. This could be related to the intrinsic properties of MnO. MnO has a low $-\Delta H_f^0$, indicating that the redox properties of MnO are excellent. Mn^{2+} can be oxidized to Mn^{3+}, Mn^{4+}, Mn^{6+} and even Mn^{7+}, and the multi-valency of $Mn^{\delta+}$ is possible in the F–T reaction. As mentioned above, the role of LTMO is to facilitate CO dissociation at the interface sites of the metal and promoter due to electronic interaction with the metal surface. The promotion of CO dissociation on the metal surface was attributed to the backdonation of electrons from Co occupied metal oribitals to the unoccupied 2π antibonding oribitals of CO, leading to a weaker C–O bond. Thus, the change of the electrostatic field caused by the variation of the valence of MnO might promote the backdonation of electrons from Co metal oribitals to the 2π oribitals of CO, resulting in an increase in the concentration of CH_x precursor and the rate of formation of F–T products while suppressing the formation of CH_4. Yin *et al.*[13] also reported that the Co catalyst with MnO promoter supported on HMS mesoporous materials showed a low

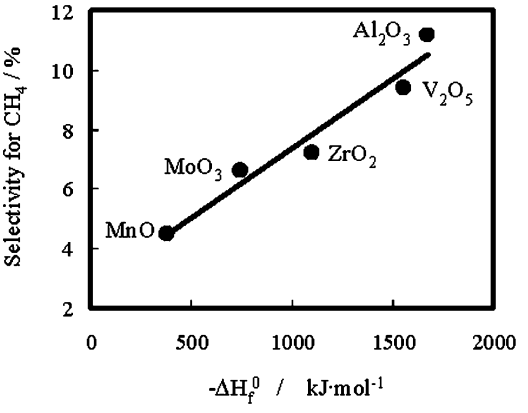

Fig. 7 The relationship between CH_4 selectivity and the standard formation enthalpy of $M^{\delta+}O$, $-\Delta H_f^0$.

View Online

selectivity for CH_4. On the contrary, Al_2O_3 has a high $-\Delta H_f^0$, indicating the invariance of the valency of Al_2O_3. As suggested above, the role of Al_2O_3 is to partially divide the active Co sites and to prevent the increase of Co particle size. Thus, Al_2O_3 is a textual promoter and its effects cannot be ascribed to electronic effects but to ensemble effects.

Conclusions

A series of mesoporous metallo-silicates (M-MPS, M = Al, Mn, V, Zr, and Mo) was used as the support of Co catalysts for F–T synthesis in the slurry phase. Compared with the purely siliceous MPS support, the catalysts supported on M-MPS materials tend to increase the selectivity for heavy hydrocarbons C_{5+} and also the chain growth probability α while restraining CH_4 selectivity. This might be attributed to metals incorporated into the silica framework. The selectivity for CH_4 can be related to the intrinsic properties of the metal oxides incorporated into the silica framework and it tends to decrease with decreasing standard enthalpy of formation of the metal oxide, $-\Delta H_f^0$.

Acknowledgements

We thank JSPS for financial support (contract No. JSPS-RFTF98P01001).

References

1 C. T. Kresge, M. E. Leonowizc, W. J. Roth, J. C. Vartuli and J. S. Beck, *Nature (London)*, 1992, **359**, 710.
2 S. C. Shen and S. Kawi, *J. Phys. Chem. B*, 1999, **103**, 8870.
3 T. Blasco, A. Corma, M. T. Navarro and J. P. Pariente, *J. Catal.*, 1995, **156**, 65.
4 P. R. H. P. Rao, A. V. Ramaswamy and P. Ratbasany, *J. Catal.*, 1992, **137**, 225.
5 D.-H. Cho, T.-S. Chang, S.-K. Ryu and Y. K. Lee, *Catal. Lett.*, 2000, **64**, 227.
6 A. Tuel, S. Gontier and R. Teissier, *Chem. Commun.*, 1996, 651.
7 L.-Z. Wang, J.-L. Shi, J. Yu and D.-S. Yan, *Nanostruct. Mater.*, 1998, **10**, 1289.
8 W. A. Garvalho, P. B. Varaldo, M. Wallau and U. Schuchardt, *Zeolites*, 1997, **18**, 408.
9 Z. Zhu, Z. Chang and L. Kevan, *J. Phys. Chem. B*, 1999, **103**, 2680.
10 A. S. Araujo and M. Jaroniec, *J. Colloid Interface Sci.*, 1999, **218**, 462.
11 S. C. Laha, P. Mukherjee, S. R. Sainkar and R. Kumar, *J. Catal.*, 2002, **207**, 213.
12 A. Tuel and S. Gontier, *Chem. Mater.*, 1996, **6**, 114.
13 D.-H. Yin, W.-H. Li, W.-S. Yang, H.-W. Xiang, Y.-H. Sun, B. Zhong and S.-Y. Peng, *Microporous Mesoporous Mater.*, 2001, **47**, 15.
14 T. Iwasaki, M. Reinikainen, Y. Onodera, H. Hayashi, T. Ebina, T. Nagase, K. Torii, K. Kataja and A. Chatterjee, *Appl. Surf. Sci.*, 1998, **130–132**, 845.
15 Y. Wang, M. Noguchi, Y. Takahashi and Y. Otsuka, *Catal. Today*, 2001, **68**, 3.
16 M.-D. Wei, K. Okabe, H. Arakawa and Y. Teraoka, *React. Kinet. Catal. Lett.*, 2002, **77**, 381.
17 M.-D. Wei, K. Okabe, H. Arakawa and Y. Teraoka, *New J. Chem.*, 2002, **26**, 20.
18 Y. Setoguchi, Y. Teraoka, I. Moriguchi and S. Kagaea, *J. Porous Mater.*, 1997, **4**, 129.
19 L. Fan, Y.-Z. Han, K. Yokota and K. Fujimoto, *Sekiyu Gakkaishi*, 1999, **39**, 111.
20 R. K. Rana and B. Viswanathan, *Catal. Lett.*, 1998, **52**, 25.
21 K. Chaudhari, R. Bal, T. K. Das, A. Chandwadkar, D. Srinivas and S. Sivasanker, *J. Phy. Chem., B*, 2000, **104**, 11 066.
22 S. C. Laha and R. Kumar, *Microporous Mesoporous Mater.*, 2002, **53**, 163.
23 R. K. Rana, A. C. Pulikottil and B. Viswanathan, *Stud. Surf. Sci Catal.*, 1998, **113**, 211.
24 B. Rakshe, V. Ramaswamy and A. V. Ramaswamy, *J. Catal.*, 1996, **163**, 501.
25 A. Corma, M. T. Navarro, J. Perez-Periente and F. Sanchez, *Stud. Surf. Sci. Catal.*, 1994, **84**, 69.
26 J. Venter, M. Kaminisky, G. L. Geoffrey and M. A. Vannice, *J. Catal.*, 1987, **103**, 450.
27 R. A. Fiato and S. L. Soled, *US Pat.* 4621102, 1986.
28 R. Karaselçuk, A. I. İşli, A. E. Aksoylu and Z. İ. Önsan, *Appl. Catal., A*, 2000, **192**, 263.
29 H. Chen and A. A. Adesina, *Appl. Catal., A*, 1994, **112**, 87.
30 A. A. Adesina, *Appl. Catal., A*, 1996, **138**, 345.
31 *CRC Handbook of Chemistry and Physics*, ed. D. R. Lide, CRC Press, Boca Raton, FL, 75th edn., 1994.

Published on 08 May 2003 on http://pubs.rsc.org | doi:10.1039/B300723P
Downloaded on 26 October 2010